Phosphorylation of inositol 1,4,5-trisphosphate receptors by protein kinase B/Akt inhibits Ca^{2+} release and apoptosis

Tania Szado*, Veerle Vanderheyden†, Jan B. Parys†, Humbert De Smedt†, Katja Rietdorf*, Larissa Kotelevets‡, Eric Chastre‡, Farid Khan§, Ulf Landegren¶, Ola Söderberg¶, Martin D. Bootman*‖, and H. Llewelyn Roderick*‖**

Laboratories of *Molecular Signaling and §Protein Technologies, The Babraham Institute, Cambridge CB2 3AT, United Kingdom; **Department of Pharmacology, University of Cambridge, Tennis Court Road, Cambridge CB2 1PD, United Kingdom; †Laboratory of Molecular and Cellular Signaling, Department of Molecular Cell Biology, Katholieke Universiteit Leuven, Campus Gasthuisberg O/N1, B-3000 Leuven, Belgium; ‡Institut National de la Santé et de la Recherche Médicale, Unite 773, Centre de Recherche Bichat Beaujon, Faculté de Médecine X. Bichat, Université Paris 7 Denis Diderot, 75018 Paris, France; and ¶Department of Genetics and Pathology/Molecular Medicine, The Rudbeck Laboratory, University of Uppsala, Se-75185 Uppsala, Sweden

Communicated by Michael J. Berridge, The Babraham Institute, Cambridge, United Kingdom, December 3, 2007 (received for review November 1, 2007)

Imbalance of signals that control cell survival and death results in pathologies, including cancer and neurodegeneration. Two pathways that are integral to setting the balance between cell survival and cell death are controlled by lipid-activated protein kinase B (PKB)/Akt and Ca^{2+}. PKB elicits its effects through the phosphorylation and inactivation of proapoptotic factors. Ca^{2+} stimulates many prodeath pathways, among which is mitochondrial permeability transition. We identified Ca^{2+} release through inositol 1,4,5-trisphosphate receptor ($InsP_3R$) intracellular channels as a prosurvival target of PKB. We demonstrated that in response to survival signals, PKB interacts with and phosphorylates $InsP_3Rs$, significantly reducing their Ca^{2+} release activity. Moreover, phosphorylation of $InsP_3Rs$ by PKB reduced cellular sensitivity to apoptotic stimuli through a mechanism that involved diminished Ca^{2+} flux from the endoplasmic reticulum to the mitochondria. In glioblastoma cells that exhibit hyperactive PKB, the same prosurvival effect of PKB on $InsP_3R$ was found to be responsible for the insensitivity of these cells to apoptotic stimuli. We propose that PKB-mediated abolition of $InsP_3$-induced Ca^{2+} release may afford tumor cells a survival advantage.

signaling | cell death | cancer

Protein kinase B (PKB) is a central player in regulating many signaling pathways controlling cell metabolism, growth, and survival (1, 2). PKB elicits these effects by phosphorylating and regulating the activity of downstream targets such as glycogen synthase kinase 3β and Bad, or via transcription factors such as Forkhead (1, 3). Because of this critical role of PKB, gain or loss of function is manifest in major disease phenotypes such as cancer and type 2 diabetes (1, 4–6).

Ca^{2+} released from the endoplasmic reticulum (ER) through inositol 1,4,5-trisphosphate ($InsP_3$) receptors ($InsP_3Rs$) plays a key role in regulating physiological processes (7). However, under pathological conditions, $InsP_3$-induced Ca^{2+} release (IICR) can be subverted to promote cell death pathways (8–10). The importance of IICR in cell death is underlined by the uncovering of functional interactions with a number of proteins with known proapoptotic and antiapoptotic activity. Notable among these are Bcl-2, Bcl-X_L, and cytochrome *c* (11–14). PKB has also recently been shown to phosphorylate the $InsP_3R$, with consequences for cell survival (15).

We investigated whether cross-talk between the phosphatidylinositol 3-kinase (PI3K)/PKB and $InsP_3/Ca^{2+}$ signaling pathways regulated how cells responded to death-inducing stimuli. We determined that PKB-mediated phosphorylation of $InsP_3R$ results in a decrease in the magnitude of IICR and resultant flux of Ca^{2+} from the ER to mitochondria. Moreover, we show that this decrease in Ca^{2+} flux caused by PKB-mediated phosphorylation of $InsP_3Rs$ contributes to protection from the effects of apoptotic stimuli. This prosurvival action of PKB was also apparent in a glioblastoma cell line (U87) that exhibits increased PKB activity caused by a deletion in the gene encoding the phosphatidylinositol 3,4,5 trisphosphate (PIP3) phosphatase, PTEN. Together, these results contribute to a mechanism by which PKB and IICR interact to regulate cell death and survival.

Results

Ca^{2+} Release from Intracellular Stores Is Regulated by PKB. Growth factor status and genetic factors that enhance PKB activity significantly impact on cell fate [supporting information (SI) Fig. 7]. On the other hand, the occurrence of Ca^{2+} signals during the cell death process, and the protection from apoptosis afforded by buffering intracellular Ca^{2+}, places Ca^{2+} at a central position in promoting cell death (SI Fig. 7).

Because of the central roles of both PKB and Ca^{2+} in regulating cell death, we investigated whether PKB-mediated phosphorylation of $InsP_3Rs$, and suppression of Ca^{2+} signals, contributed to the prosurvival role of PKB. Inducible overexpression of constitutively active PKB (CA-PKB) promoted the phosphorylation of $InsP_3Rs$ (Fig. 1*A* and SI Fig. 8 for characterization of CA-PKB-expressing cell lines). The example Ca^{2+} traces and the histogram of the percentage of responding cells in Fig. 1 *Bi* and *Bii*, respectively, illustrate the significant inhibition of histamine-induced Ca^{2+} release by CA-PKB overexpression. The time from agonist addition to peak response (latency) and the percentage of cells exhibiting Ca^{2+} oscillations after application of 100 μM histamine was also reduced in CA-PKB-expressing cells (SI Fig. 9 *Ai* and *Aii*). Kinase dead (KD)-PKB had no effect on agonist-induced Ca^{2+} signals (Fig. 1*B* and SI Fig. 9*A*). Ca^{2+} release stimulated by cell permeant $InsP_3$ ($InsP_3$-BM) was also reduced by CA-PKB overexpression, indicating that PKB was directly modulating IICR (Fig. 1*C* and SI Fig. 9*B*). The PKB-mediated inhibition of agonist-induced Ca^{2+} release was not caused by a decrease in ER luminal Ca^{2+} content because the integrated cytosolic Ca^{2+} transient [area under the curve (AUC)] induced by the irreversible sarco/ER ATPase (SERCA) pump inhibitor thapsigargin was unaffected by CA-PKB expression (29,860 ± 1,118 nM·s vs. 31,220 ± 767.7 nM·s; $P > 0.05$ in YFP- or CA-PKB-expressing cells, respectively).

Author contributions: T.S., V.V., J.B.P., H.D.S., M.D.B., and H.L.R. designed research; T.S., V.V., K.R., M.D.B., and H.L.R. performed research; K.R., L.K., E.C., F.K., U.L., O.S., and H.L.R. contributed new reagents/analytic tools; T.S., V.V., J.B.P., H.D.S., M.D.B., and H.L.R. analyzed data; and M.D.B. and H.L.R. wrote the paper.

The authors declare no conflict of interest.

‖To whom correspondence may be addressed: E-mail: martin.bootman@bbsrc.ac.uk or llewelyn.roderick@bbsrc.ac.uk.

This article contains supporting information online at www.pnas.org/cgi/content/full/0711324105/DC1.

© 2008 by The National Academy of Sciences of the USA

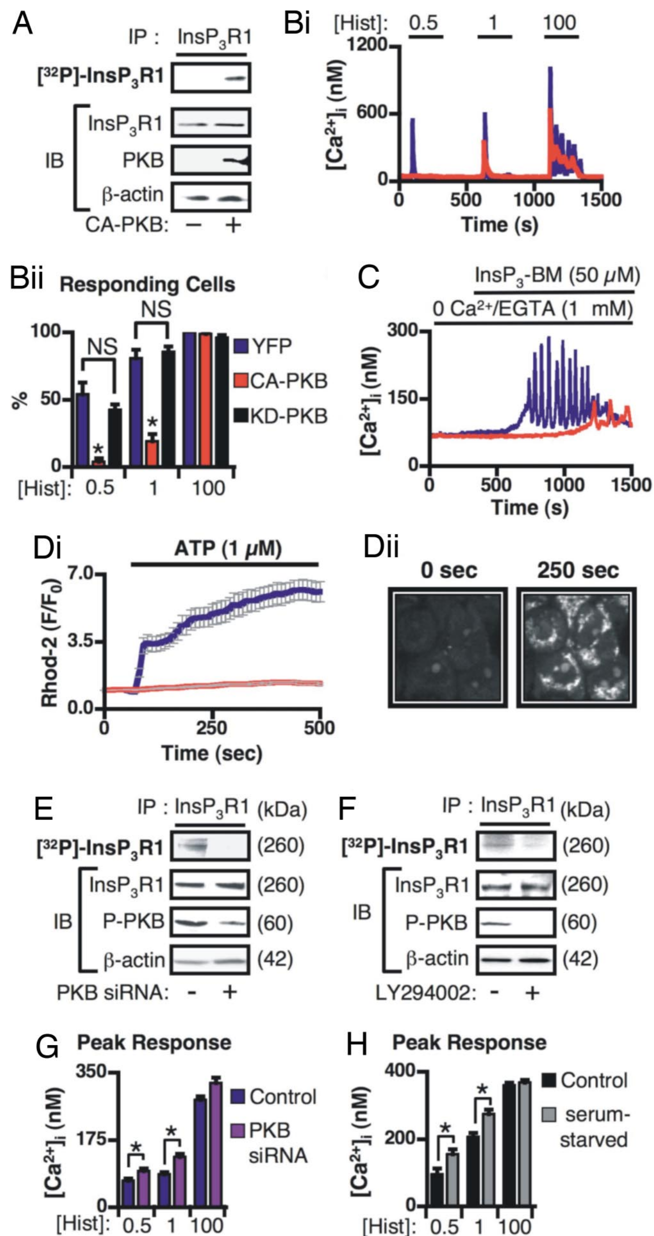

Fig. 1. IICR and mitochondrial Ca^{2+} uptake is regulated by PKB. (*A*) CA-PKB expression promotes phosphorylation of $InsP_3R1$. (*Upper*) An autoradiograph of ^{32}P-labeled $InsP_3Rs$. (*Lower*) Immunoblots (IB) of proteins present in the lysates used as input for the IPs. $InsP_3Rs$ were immunoprecipitated from control cells (−) or cells expressing CA-PKB as shown (+). (*Bi* and *Bii*) Histamine-induced Ca^{2+} signals in HeLa cells expressing CA-PKB ($n = 89$ cells), YFP ($n = 64$ cells), or KD-PKB ($n = 74$ cells). (*Bi*) Typical responses from individual HeLa cells stimulated with the histamine concentrations (μM) shown. (*Bii*) Averaged data showing the effect of CA-PKB or KD-PKB expression on the proportion of responding cells. (*C*) Typical Ca^{2+} responses recorded in control and CA-PKB-expressing cells stimulated with $InsP_3$ ester ($InsP_3$-BM). (*Di*) Average background subtracted, mitochondrial Rhod-2 fluorescence changes in control and CA-PKB expressing HeLa cells. (*Dii*) Confocal images of Rhod-2 fluorescence in HeLa cells stimulated with 1 μM ATP. Images captured at the indicated time points are shown. (*E* and *F*) (*Upper*) Autoradiographs of ^{32}P-labeled $InsP_3Rs$. (*Lower*) Immunoblots (IB) of the indicated proteins in the lysates used as input for the IPs. (*E*) $InsP_3R$ phosphorylation in HeLa cell transfected with PKB siRNA or control siRNA. (*F*) Effect of LY294002 on$InsP_3R$ phosphorylation in HeLa cells grown under serum-replete normal growth conditions. (*G*) Impact of PKB siRNA or control siRNA on the amplitude of Ca^{2+} responses induced by the concentrations of histamine (μM) indicated. (*H*) Amplitude of Ca^{2+} responses induced by the concentrations of histamine (μM) shown in control and serum-starved HeLa cells. The data represent mean ± SEM. * indicates $P < 0.05$. NS indicates not significant.

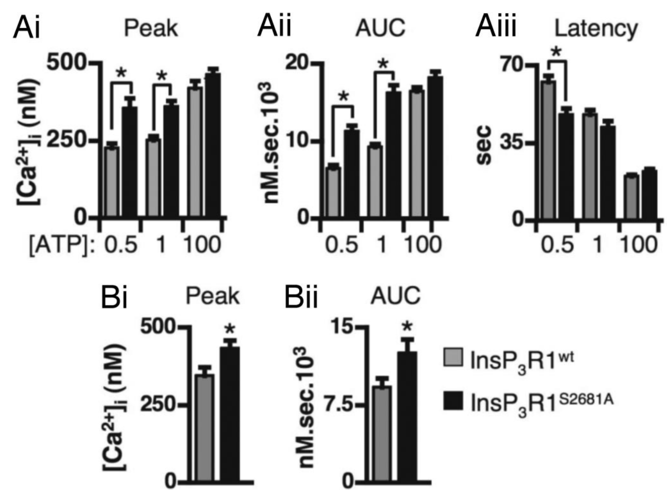

Fig. 2. $InsP_3R1$-S2681 regulates agonist-induced Ca^{2+} release. (*A i–iii*) Averaged data of ATP-induced Ca^{2+} signals in COS-7 cells expressing $InsP_3R1^{wt}$ ($n = 293$ cells) or $InsP_3R1^{S2681A}$ ($n = 192$ cells). Peak Ca^{2+} response (*Ai*), AUC (*Aii*), and latency (*Aiii*) are shown for the ATP concentrations (μM) indicated. (*B i and ii*) Carbachol-induced Ca^{2+} responses in M3-expressing DT40 cells transiently transfected with $InsP_3R1^{wt}$ ($n = 35$ cells) or $InsP_3R1^{S2681A}$ ($n = 44$ cells). * indicates that the data are statistically significant ($P < 0.05$).

As Ca^{2+} released from $InsP_3Rs$ is taken up in a privileged manner by mitochondria, mitochondrial Ca^{2+} levels represent an exquisitely sensitive measure of Ca^{2+} released from ER-localized $InsP_3Rs$. Using confocal imaging of mitochondrially compartmentalized Rhod-2 (16), a significantly lower level of agonist-induced mitochondrial Ca^{2+} uptake was observed in CA-PKB-expressing cells compared with controls (Fig. 1 *Di* and *Dii*).

Because serum-starvation sensitized cells to apoptotic stimuli (SI Fig. 7), we investigated whether $InsP_3Rs$ were phosphorylated under normal serum-replete growth where PKB is tonically active. Reduction of PKB expression by siRNA, or activity, using LY294002 (inhibits PI3K, which lies directly upstream of PKB) significantly decreased ^{32}P-labeling of $InsP_3Rs$ to a level that was not detectable above background (Fig. 1 *E* and *F*).

The tonic activity of endogenous PKB also regulated agonist-induced Ca^{2+} release. As would be expected of an $InsP_3R$ inhibitor, reduction of endogenous PKB expression by siRNA, or its activity by serum starvation, resulted in an enhancement of agonist-induced Ca^{2+} release (Fig. 1 *G* and *H*). Together, these data suggest that phosphorylation of $InsP_3R$ by PKB significantly reduces its sensitivity to $InsP_3$. Moreover, $InsP_3Rs$ are phosphorylated by endogenous, tonically active PKB (in serum), CA-PKB, and PKB that had been activated by physiological stimuli.

S2681 in $InsP_3R1$ Regulates IICR. To further isolate the contribution of PKB phosphorylation of $InsP_3Rs$ to Ca^{2+} release, IICR was quantitated in cells overexpressing $InsP_3Rs$ in which the phosphorylatable serine in the PKB consensus site was mutated to an unreactive alanine (S2681A in $InsP_3R1$) (15). COS-7 cells expressing $InsP_3R1^{S2681A}$ had greater ATP-induced Ca^{2+} responses than their $InsP_3R1^{wt}$-expressing counterparts (Fig. 2*Ai*, *Aii*, and *Aiii*; the peak, AUC, and latency of the Ca^{2+} signal are shown). These effects were not caused by differences in expression levels of the wild-type or mutated receptors or differences in their intracellular distribution (SI Figs. 10*B* and 11 and data not shown). COS-7 cells were used for these experiments because they express low levels of endogenous $InsP_3R1$ and have been successfully used to study $InsP_3R$ function (17). Moreover, in these cells, heterologously expressed wild-type $InsP_3Rs$ can be overexpressed at a level significantly greater than endogenous receptors, are correctly tar-

geted, and exhibit significantly increased agonist-induced Ca^{2+} release and decreased latency of the Ca^{2+} transient (SI Fig. 11).

Agonist-induced Ca^{2+} release was also monitored in M3 muscarinic receptor-expressing DT40 $InsP_3R$ triple knockout chicken B lymphocyte cell line (DT40 TKO) (18). The peak and AUC of the Ca^{2+} signal induced by carbachol was significantly greater in cells transiently transfected with $InsP_3R1^{S2681A}$ than cells transfected with $InsP_3R1^{wt}$ (Fig. 2 *Bi* and *Bii*). Together, the data derived from HeLa (Fig. 1), COS-7, and DT40 cells support the conclusion that phosphorylation of $InsP_3R1$-S2681 by PKB was inhibitory to Ca^{2+} release.

PKB Interacts with $InsP_3R1$. Because protein kinases often reside in a complex with their substrates, whether PKB and $InsP_3Rs$ interact was next investigated. Using coimmunoprecipitation (co-IP), an interaction between overexpressed CA-PKB and endogenous full-length $InsP_3Rs$ was detected in HeLa cells (Fig. 3 *Ai* and *Aii*). KD-PKB did not interact with $InsP_3R1$ (data not shown). PKB also interacted with a YFP-tagged ER-localized NH_2-terminally truncated $InsP_3R1$ that encompassed only the amino acids COOH-terminal of transmembrane domains 5 (YFP-CT) (Fig. 3*B*).

Because PKB is activated at the plasma membrane, but the majority of $InsP_3Rs$ reside on the ER, we next set out to establish whether activated endogenous PKB could gain access to $InsP_3Rs$ on the ER. Using an *in situ* proximity ligation assay (19), a significant $InsP_3R$-PKB interaction was detected in cells grown under serum-replete normal growth conditions (see images and histogram of mean cellular fluorescence intensity, Fig. 3 *Ci* and *Cii*). An insulin-dependent increase in PKB-$InsP_3R1$ interaction was also detected (Fig. 3 *Ci* and *Cii*). Controls that either included the $InsP_3R$ antibody immunizing peptide in the staining procedure or replacing the PKB probe with a probe for the Max protooncogene were negative (Fig. 3*Cii*). Colocalization analysis revealed that the sites where PKB and $InsP_3R1$ interacted [rolling circle amplification (RCA) product present] overlapped with the distribution of calnexin, and therefore were localized to the ER (Pearson's correlation coefficient = 0.44 ± 0.01). Using classical colocalization analysis of confocal images of immunostained cells, we found that the distribution of both total and phosphorylated active PKB also overlapped with endogenous $InsP_3Rs$ (SI Fig. 12). Together, these data show that active PKB is present not only at the plasma membrane where it is activated, but is also localized in the cytosol, where it interacts with $InsP_3Rs$.

Phosphorylation of $InsP_3Rs$ by PKB Inhibits Apoptosis. To specifically test the role of PKB-dependent phosphorylation of $InsP_3Rs$ onapoptosis, menadione-induced apoptosis was measured in COS-7 cells expressing either $InsP_3R1^{wt}$ or $InsP_3R^{S2681A}$. This cell death stimulus was used because its action was sensitive to $InsP_3$-metabolizing 5′-phosphatase expression and therefore is IICR-dependent (Fig. 4*Ai*). Cells expressing $InsP_3R1^{S2681A}$ exhibited significantly higher levels of menadione-induced apoptosis than cells expressing $InsP_3R1^{wt}$ (Fig. 4*Aii*). A similar effect was also observed when staurosporine was used to induce apoptosis (SI Fig. 13).

We next tested the idea that PKB-mediated regulation of $InsP_3R$ activity and Ca^{2+} flux from the ER to the mitochondria contributed to the mechanism by which PKB elicited its prosurvival effects. Significantly, menadione-induced mitochondrial Ca^{2+} increases were considerably reduced in cells overexpressing $InsP_3R1^{S2681A}$, but not cells expressing $InsP_3R1^{wt}$ (Fig. 4*B*).

PKB Regulation of IICR and Apoptosis in Glioblastoma Cells. Many cancers exhibit increased PKB activity as a result of mutation or deletion of the gene encoding the lipid phosphatase PTEN (6). This mechanism underlies the resistance to apoptotic stimuli of the U87 glioblastoma cell line (20). Re-expression of PTEN in these cells ($U87^{PTEN}$) decreases PKB activity (Fig. 5*A*) and rescues their sensitivity to an apoptotic stimulus (SI Fig. 14). We investigated whether $InsP_3R$ was a target for the prosurvival effect of enhanced PKB activity in these cells. $InsP_3R1$ immunoprecipitated from U87 cells were more highly phosphorylated than similarly treated $U87^{PTEN}$ cells (Fig. 5*B*). IICR, stimulated by endothelin (ET), was lower in U87 cells than in $U87^{PTEN}$ cells (Fig. 5*C*). Furthermore, mitochondrial Ca^{2+} increases after exposure to menadione were significantly lower in the U87 cells than the $U87^{PTEN}$ cells (Fig. 5*D*). Both menadione–induced mitochondrial Ca^{2+} uptake and apopto-

Fig. 3. PKB interacts with $InsP_3R1$. (*A i* and *ii*) Co-IPs of full-length $InsP_3R1$ with PKB. A line is shown in the images where different parts of the same gel have been grouped. (*Ai*) IPs using anti-$InsP_3R1$ antibody or preimmune IgG were performed on lysates prepared from HeLa cells expressing YFP or CA-PKB. (*Aii*) Immunoblot showing the proteins present in the lysates used as input for the IP in *Ai*. (*B*) Co-IP of PKB with the $InsP_3R1$ COOH terminus. IPs using anti-GFP antibody or preimmune IgG control from lysates prepared from cells transfected with YFP-CT and/or CA-PKB DNA. (*Top*) An immunoblot (IB) to detect co-IP of PKB. (*Middle* and *Bottom*) Immunoblots of the proteins present in the lysates used for IP. (*C i* and *ii*) *In situ* proximity ligation assay in HeLa cells. (*Ci*) The red pseudocoloration indicates an interaction between endogenous $InsP_3R1$ and PKB. The ER is indicated by the CLNX staining in green. Nuclei are shown by the blue DAPI staining. (*Cii*) Quantitation of proximity ligation assay ($n = 50$ cells per condition). The bars represent the mean intensity ± SEM of AlexaFluor 561 fluorescence. * denotes that the data are significantly different ($P < 0.05$).

CELL BIOLOGY

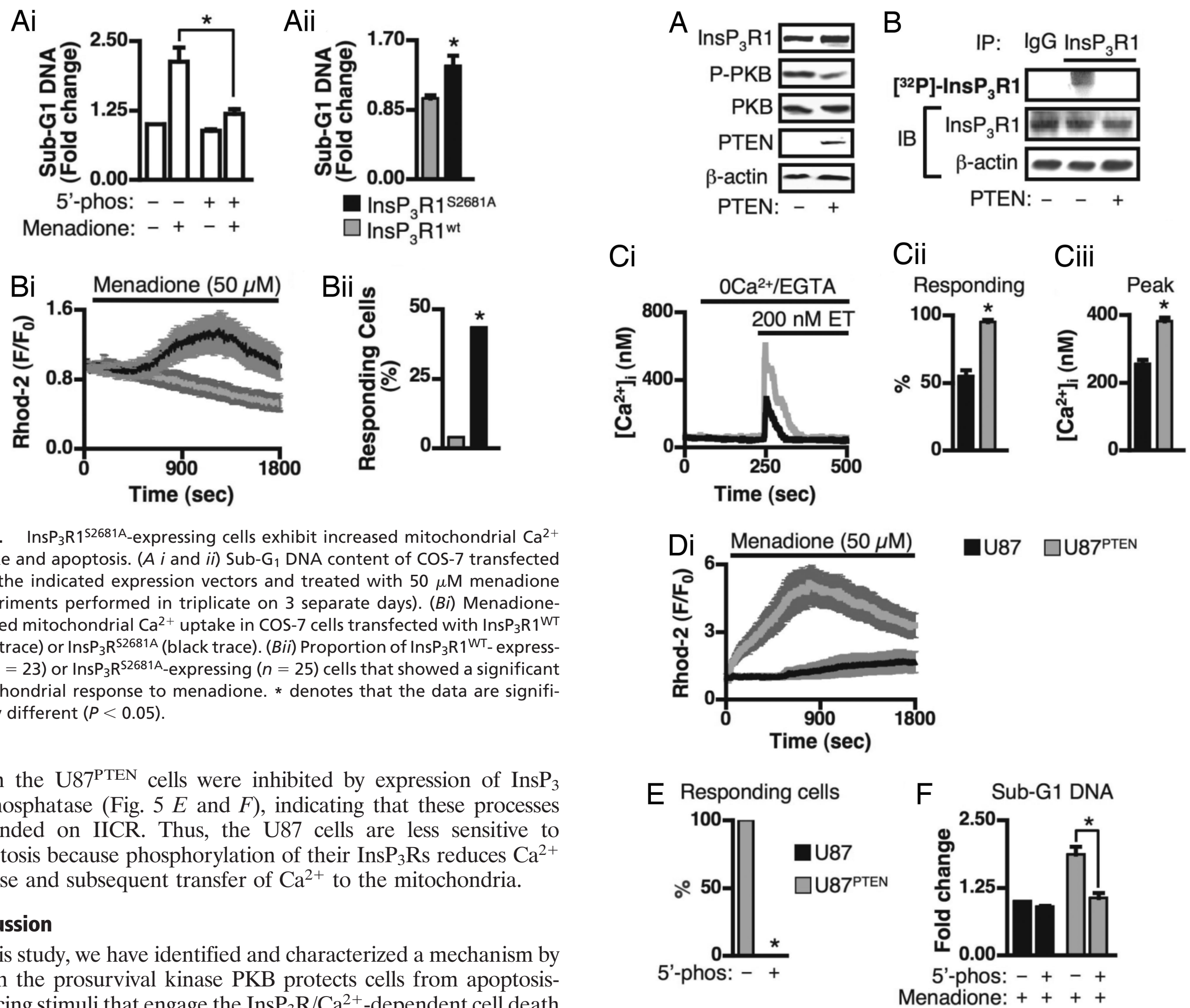

Fig. 4. $InsP_3R1^{S2681A}$-expressing cells exhibit increased mitochondrial Ca^{2+} uptake and apoptosis. (*A i* and *ii*) Sub-G_1 DNA content of COS-7 transfected with the indicated expression vectors and treated with 50 μM menadione (experiments performed in triplicate on 3 separate days). (*Bi*) Menadione-induced mitochondrial Ca^{2+} uptake in COS-7 cells transfected with $InsP_3R1^{WT}$ (gray trace) or $InsP_3R^{S2681A}$ (black trace). (*Bii*) Proportion of $InsP_3R1^{WT}$- expressing (n = 23) or $InsP_3R^{S2681A}$-expressing (n = 25) cells that showed a significant mitochondrial response to menadione. * denotes that the data are significantly different ($P < 0.05$).

Fig. 5. $InsP_3R$ phosphorylation results in decreased agonist-induced Ca^{2+} release and menadione-induced mitochondrial Ca^{2+} uptake in PTEN-deficient, U87 glioblastoma cells. (*A*) Immunoblots of the indicated proteins in lysates prepared from U87 and $U87^{PTEN}$ cells (indicated by PTEN − and +, respectively). (*B*) (*Top*) Autoradiograph of ^{32}P-labeled $InsP_3Rs$ immunoprecipitated from U87 and $U87^{PTEN}$ cells. (*Middle* and *Bottom*) The proteins present in the lysate used as input for the IP. (*C i–iii*) ET-induced Ca^{2+} release in U87 cells (black; n = 190 cells) and $U87^{PTEN}$ cells (gray; n = 183 cells). (*Ci*) Typical traces of ET-induced Ca^{2+} release in U87 and $U87^{PTEN}$ cells. (*Cii*) Proportion of responding cells. (*Ciii*) Peak Ca^{2+} response. (*Di*) Menadione-induced mitochondrial Ca^{2+} uptake in U87 cells (black trace; n = 25) and $U87^{PTEN}$ cells (gray trace; n = 14). (*E*) Proportion of YFP-expressing (n = 50) and $InsP_3$ 5′-phosphatase-expressing (n = 50) $U87^{PTEN}$ cells that exhibited menadione-induced increases in mitochondrial Ca^{2+}. (*F*) Menadione-stimulated cell death in $U87^{PTEN}$ cells depended on $InsP_3Rs$. U87 and $U87^{PTEN}$ cells were adenovirally infected with $InsP_3$ 5′-phosphatase or YFP, and subsequently stimulated with 50 μM menadione (experiments performed in triplicate on 3 separate days). * indicates that the data are significantly different ($P < 0.05$).

sis in the $U87^{PTEN}$ cells were inhibited by expression of $InsP_3$ 5′-phosphatase (Fig. 5 *E* and *F*), indicating that these processes depended on IICR. Thus, the U87 cells are less sensitive to apoptosis because phosphorylation of their $InsP_3Rs$ reduces Ca^{2+} release and subsequent transfer of Ca^{2+} to the mitochondria.

Discussion

In this study, we have identified and characterized a mechanism by which the prosurvival kinase PKB protects cells from apoptosis-inducing stimuli that engage the $InsP_3R/Ca^{2+}$-dependent cell death pathway. We also provide evidence for a fundamental role of this mechanism in regulating the sensitivity of a cancer cell line to apoptotic stimuli.

The data presented here shows that agonist-induced Ca^{2+} release is inhibited by PKB-mediated phosphorylation of $InsP_3Rs$. Significantly, agonist-induced Ca^{2+} release was regulated by endogenous tonically active PKB and CA-PKB that had been overexpressed. Moreover, increased cellular PKB activity significantly impacted the agonist-induced increase in mitochondrial Ca^{2+}, which is a proximal sensor of Ca^{2+} release through $InsP_3Rs$ (21, 22). Because PKB activation had no effect on ER store loading or $InsP_3R$ expression levels, but prevented Ca^{2+} release in response to cell-permeant $InsP_3$, we concluded that PKB was directly regulating $InsP_3R$ activity. This conclusion was further supported by the enhanced agonist-induced Ca^{2+} release observed in cells expressing mutated $InsP_3Rs$ that could not be phosphorylated by PKB compared with cells overexpressing wild-type receptors.

The data presented here contrasts with that previously reported by Khan *et al.* (15), which indicated that mutation of S2681A did not affect IICR. Possible explanations for these discrepancies are that in the study of Khan *et al.* increases in intracellular Ca^{2+} were presented as a normalized change in fluorescence but not absolute Ca^{2+} values. Thus, they could only conclude that there was no effect of $InsP_3R1$ S2681 phosphorylation on the EC_{50} for Ca^{2+} release. A further possibility is that because of the low tonic level of PKB activity in DT40 cells (SI Fig. 15 and ref. 23), the wild-type $InsP_3R$ would not have been highly phosphorylated, and thus the effect of $InsP_3R1^{S2681A}$ would have been small. Unlike Khan *et al.* (15), we were able to detect a small, but significant, effect of the S2681A mutation on Ca^{2+} release in DT40 cells, although it was less than that observed in COS-7 cells. A possible explanation for our ability to detect an effect of S2681A mutation upon Ca^{2+} release is that unlike Khan *et al.*, we used DT40 cells stably expressing muscarinic receptors rather than cells in which muscarinic receptors were transiently transfected.

Our data show that during the life cycle of normally dividing cells $InsP_3Rs$ are tonically phosphorylated by PKB. Stimulation of serum-starved cells with insulin or FBS also promoted PKB-dependent phosphorylation of $InsP_3Rs$ (SI Fig. 10*A*). Experiments performed here also corroborated the identification of S2681 as the serine residue phosphorylated by PKB in $InsP_3R1$ by Khan *et al.* (15) (SI Fig. 10 *B* and *C*) and demonstrated that S2681 was the site for phosphorylation by endogenous PKB that had been physiologically activated. We also showed *in vitro* phosphorylation of this site in recombinant $InsP_3R1$ COOH terminus by recombinant PKB, indicating that PKB was sufficient to catalyze the phosphorylation of $InsP_3Rs$, and that no accessory factors are required. We report that $InsP_3R3$ is also phosphorylated by PKB, both *in vitro* by recombinant active PKB (SI Fig. 10*D*) and after insulin stimulation in intact cells (data not shown). Together, our data satisfies the criteria laid out by Manning and Cantley (1) for a protein to constitute a PKB substrate. Interestingly, in the absence of activated PKB, no $InsP_3R$ phosphorylation was observed. Because $InsP_3Rs$ are a substrate for a number of other protein kinases, including PKA and CaMKII (24, 25), it might be expected that basal activity of these enzymes may also lead to a low level of phosphorylation of $InsP_3R1$. However, in the studies cited above, it appears that unless stimulated appropriately little $InsP_3R$ phosphorylation is detected. The remarkable degree of sequence conservation through evolution of the PKB consensus site in $InsP_3Rs$ is suggestive of a fundamental role of phosphorylation of this region in $InsP_3R$ function. The COOH terminus of $InsP_3Rs$ is critically important in the regulation of channel gating and is a hotspot for interactions with other proteins, including huntingtin-associated protein, Bcl-X_L, protein phosphatase 1a, and cytochrome *c* (12, 14, 26–28). Akin to other protein kinases/substrate relationships (29), we also detected an interaction between PKB and the $InsP_3R$. Using an *in situ* proximity ligation technique, we detected this interaction between endogenous PKB and $InsP_3Rs$ in cells either maintained in serum-containing medium or stimulated with insulin. Significantly, this PKB–$InsP_3R$ association occurred throughout the ER, and not only at the plasma membrane where PKB is primarily activated. Activated PKB was, however, detected throughout the cell. Although PIP_3 has previously been localized to the ER (30), we have shown a clear visualization of endogenous activated PKB interacting with one of its substrates in a location distal from the plasma membrane.

By investigating the effect of mutagenesis of the PKB consensus site in $InsP_3R1$ on cell death and mitochondrial Ca^{2+} increases stimulated by agents that cause apoptosis in an IICR-dependent manner (14, 31), we also determined that IICR was a bona fide prosurvival target of PKB. The relevance of these findings to disease was shown in the U87 glioblastoma cancer cell line that exhibits increased PKB activity (20). In these cells, we detected increased $InsP_3R$ phosphorylation and decreased agonist-induced Ca^{2+} release when compared with derivatives of these cells in which PTEN was re-expressed. Furthermore, unlike their PTEN-expressing derivatives, the U87 cells were also recalcitrant to menadione-induced apoptosis and did not exhibit any mitochondrial Ca^{2+} uptake after menadione treatment. From these data we conclude that phosphorylation of $InsP_3Rs$ by hyperactive PKB was significantly responsible for the lack of sensitivity of the U87 cells to apoptotic stimuli.

In summary, we provide evidence for a mechanism by which $InsP_3R$-mediated apoptosis is inhibited and by which PKB elicits its prosurvival effects (Fig. 6). This model also predicts that PKB constitutes a link between the cellular environment and growth factor status and can dynamically control IICR to determine cell fate. The significant prosurvival effect of PKB-mediated phosphorylation of $InsP_3Rs$ places regulation of IICR high up in the hierarchy of the prosurvival targets of PKB. Indeed, IICR is an upstream signal in the activation of other proapoptotic pathways such as those mediated by Bad and calpains (9). Although our data focus on the role of PKB modulation of IICR in apoptosis, it is likely that this functional interaction also impacts other aspects of Ca^{2+} signaling. The recent descriptions of role for IICR in controlling autophagy (32) and cellular metabolism (12), which are also targets for the PKB pathway, support this idea. In addition, our data contribute to the developing model that regulation of IICR is a nexus at which multiple signaling pathways converge to determine the physiological output of a given cellular stimulus.

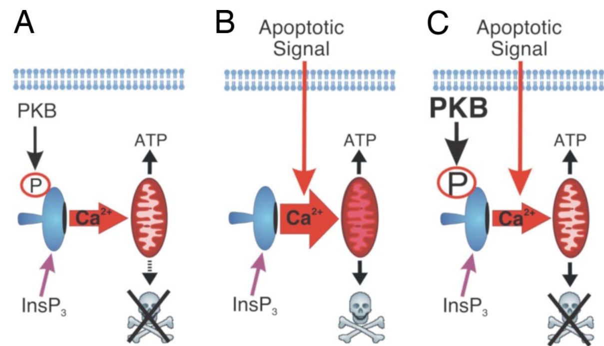

Fig. 6. Model depicting the functional interaction between PKB and $InsP_3Rs$. (*A*) Under normal growth conditions with physiological PKB activity $InsP_3Rs$ are basally phosphorylated, transfer of Ca^{2+} to the mitochondria is minimal, and ATP synthesis is promoted. (*B*) In the absence of growth factors, PKB activity is reduced, and the level of $InsP_3R$ phosphorylation is diminished. Thus, upon toxin application Ca^{2+} flux from the ER to the mitochondria is enhanced, causing permeability transition and cell death. (*C*) In situations with enhanced PKB activity, such as during cancer or the presence of growth factor stimulation, the level of $InsP_3R$ phosphorylation is increased, thereby decreasing the flux of Ca^{2+} from the ER to the mitochondria in response to an apoptotic stimulus. Agonist-induced Ca^{2+} release is also suppressed under these conditions.

Materials and Methods

Materials. Cell culture reagents, NuPage gels, AlexaFluor-conjugated secondary antibodies, Ca^{2+} indicator dyes, and pluronic were from Invitrogen. Blasticidin, Zeocin, and tetracycline-free FBS were from InvivoGen. Primary antibodies, unless otherwise stated, were from Cell Signaling Technology. All other chemicals, unless stated otherwise, were purchased from Sigma.

Generation of Expression Vectors. Expression plasmids for myristoylated CA and KD (K179A) forms of PKB have been described (33). The cDNAs encoding CA-PKB and KD-PKB were subcloned into the tetracycline-inducible expression vector pcDNA4-TO (Invitrogen), and pcDNA4-TO-YFP was created by subcloning the YFP cDNA from pEYFP-C1 (Clontech) into pcDNA4-TO. $InsP_3R1^{S2681A}$ was generated by QuikChange Mutagenesis (Stratagene) using pcDNA3-mouse $InsP_3R1$ (provided by K. Mikoshiba, University of Tokyo, Tokyo) as template. The COOH-terminal mutant S2681A ($CT^{S/A}$) was made as above. Constructs were verified by sequencing. YFP-tagged $InsP_3R1$ COOH terminus (YFP-CT; amino acids 2431–2749) has been described (34).

Generation of Stable Cell Lines. Tet suppressor HeLa cells were from Invitrogen and maintained as prescribed. Stable PKB- and YFP-expressing cell lines were generated after transfection by using GeneJuice (Merck) or JetPEI (Qbiogene) according to the manufacturer's guidelines. Expression was induced with 1 μg/ml doxycycline for 24 h.

Transient Transfection. HeLa and COS-7 cell lines were from ECACC and maintained as described (35). For knockdown of endogenous PKB, cells were transfected with validated siRNA (Cell Signaling Technology) by using Lipofectamine 2000 (Invitrogen). Scrambled siRNA was used as control. For DNA transfection, Lipofectamine 2000 or JetPei (Qbiogene) was used. For imaging studies, $InsP_3R$ transfected cells were identified by cotransfection with pEYFP-C1 (Clontech) at a 1:5 molar ratio. GFP-tagged $InsP_3$ 5′-phosphatase was transduced by using adenovirus. Cells were infected at a multiplicity of infection of 100 plaque-forming units 24 h before analysis or treatment. A GFP-expressing adenovirus was used as control. Adenoviral vectors were prepared according to the supplier's instructions (Microbix). M3-muscarinic receptor-expressing DT40 $InsP_3R$ triple knockout chicken B-lymphocytes were from David Yule (University of Rochester, Rochester, NY) and cultured as described (18). DT40 cells were transfected with an AMAXA

Nucleofector with solution T and program B-023. In brief, 2×10^6 cells were first resuspended in 100 μl of solution T. To the cells in solution T, 10 μg of empty vector or $InsP_3R1$ expression vector was added together with 3 μg of a DsRed expression vector, which was used a transfection marker.

Ca^{2+} Imaging. Fura-2 imaging was performed as described (35). Experiments were performed on three coverslips of 20 or more cells per day on 3 separate days. Mitochondrial Ca^{2+} imaging with Rhod-2 was performed as described (16). Experiments were performed by using a VoxCell Scan confocal imaging system (Visitech Ltd) equipped with a Hamamatsu ORCA-ER camera. The confocal scan head was attached to either an Olympus IX70 inverted microscope configured with a $\times$40, 1.35 n.a. UAPO oil immersion objective (Figs. 4 and 5) or a Nikon TE2000 equipped with $\times$40, 1.3 n.a. oil immersion objective (Fig. 1). Image analysis was performed with ImageJ.

Immunoblotting. Immunoblots were performed essentially as described (35). For detection of PKB, 15–40 μg of cell lysate was separated on 7% or 10% SDS/PAGE or 4–12% precast Bis-Tris NuPAGE gradient gels. Proteins were detected with polyclonal or monoclonal PKB antibodies (both diluted 1:1,000). β-Actin was used as a loading control (mAb 1:10,000; Abcam). Phospho-PKB (S473) (1:1,000) was detected after stripping of total PKB antibody. $InsP_3R1$ was detected by using a polyclonal antibody generated in house against the COOH terminus of the protein as described (36).

^{32}P Labeling of $InsP_3Rs$. Labeling experiments were performed similar to that described (35). In this study, 300 μg of protein lysate prepared from 2 $\times$ 35-mm dishes per condition was used for IP.

***In Situ* Proximity Ligation Assay.** This assay was performed as described (19). Proximity probes were constructed by conjugating oligonucleotides to a monoclonal PKB antibody and a polyclonal $InsP_3R1$ antibody. A probe for the Max oncogenic transcription factor has been described (19) and was used as a control. Cells were counterstained with an anticalnexin (CLNX) polyclonal antibody (Sigma) and visualized by using an AlexaFluor 488-conjugated secondary antibody. Coverslips were mounted in Vectashield containing DAPI (blue) (Vector Laboratories). Images were captured with a Zeiss LSM 510 META confocal microscope using a plan apochromat $\times$60, 1.40 n.a. oil immersion objective configured with LSM software version 3.2. Cellular RCA products were quantitated with ImageJ. To this end, mean pixel intensity of region of interest of the image not covered by a cell was subtracted from the mean pixel intensity of a region of interest that was drawn around each cell. The data are presented as mean pixel intensity. The brightness of sample images was increased for presentation. Pearson's colocalization analysis was performed with Volocity software using the region of interest threshold option (37) (version 4.01; Improvision).

Co-IP of $InsP_3Rs$ and PKB. Lysates were prepared as for immunoblotting. Thirty micrograms of each lysate was retained for immunoblot analysis, and IPs were performed on 500–1,000 μg of the remaining protein as described (35). $InsP_3Rs$, YFP-tagged proteins, and PKB were immunoprecipitated by using 2 μl of anti-$InsP_3R1$ or anti-GFP polyclonal antibodies or 2 μl of monoclonal PKB antibody, respectively.

Induction of Apoptosis and FACS Analysis. When experiments involved transfection or adenoviral infection, growth media were replaced with fresh media or media containing apoptosis-inducing agent after 24 h. Cells were treated for 6 h with 50 μM Menadione. Cells in the media were retained and pooled with remaining adherent cells that were harvested by trypsinization. Cells were collected by centrifugation at 1,200 $\times$ g for 5 min and fixed in 70% EtOH/PBS overnight. Cells were then pelleted, incubated for 1 h at 37°C in 600 μl of propidium iodide (PI) buffer (PBS, pH 7.4, 0.4 μg/ml PI, 0.4 μg/ml RNaseA, 0.3% IGEPAL), and analyzed by FACS. Data are presented as fold changes in sub-G_1 population compared with the experimental condition indicated.

Data Analysis. Statistical analysis was calculated by using Student's t test, ANOVA, and posthoc Tukey test or χ^2 test. Data are presented as mean $\pm$ SEM. Significance was accepted at $P < 0.05$.

ACKNOWLEDGMENTS. We thank Profs. K. Mikoshiba, C. Erneux (University of Brussels, Brussels, Belgium), C. Taylor (University of Cambridge), and B. Burgering (University Medical Center of Utrecht, Utrecht, The Netherlands) for cDNAs; Stuart Conway (University of St. Andrews, St. Andrews, Scotland) for InP_3-BM, J. Hanson, E. Vermassen, G. Morgan, S. Walker, S. Cook, L. Bauwens, M. Taussig, C. Taylor, and Y. Sun for help and discussion; and the Engineering and Physical Sciences Research Council Mass Spectrometry service (Swansea, U.K.). This work was supported in part by Fonds Wetenschappelijk Onderzoek-Vlaanderen Grant 3.0207.99, Program on Interuniversity Poles of Attraction (Belgian Science Policy) Grant P5/05, Concerted Actions of the Katholieke Universiteit Leuven Grant 99/08, The Babraham Institute, The Royal Society, Human Frontier Science Program, and Biotechnology and Biological Sciences Research Council Grant C19767.

1. Manning BD, Cantley LC (2007) AKT/PKB signaling: Navigating downstream. *Cell* 129:1261–1274.
2. Hanada M, Feng J, Hemmings BA (2004) Structure, regulation, and function of PKB/AKT: A major therapeutic target. *Biochim Biophys Acta* 1697:3–16.
3. Brunet A, Datta SR, Greenberg ME (2001) Transcription-dependent and -independent control of neuronal survival by the PI3K-Akt signaling pathway. *Curr Opin Neurobiol* 11:297–305.
4. Thompson JE, Thompson CB (2004) Putting the rap on Akt. *J Clin Oncol* 22:4217–4226.
5. Luo J, Manning BD, Cantley LC (2003) Targeting the PI3K-Akt pathway in human cancer: Rationale and promise. *Cancer Cell* 4:257–262.
6. Leslie NR, Downes CP (2004) PTEN function: How normal cells control it and tumor cells lose it. *Biochem J* 382:1–11.
7. Berridge MJ, Lipp P, Bootman MD (2000) The versatility and universality of calcium signaling. *Nat Rev Mol Cell Biol* 1:11–21.
8. Szalai G, Krishnamurthy R, Hajnoczky G (1999) Apoptosis driven by IP_3-linked mitochondrial calcium signals. *EMBO J* 18:6349–6361.
9. Orrenius S, Zhivotovsky B, Nicotera P (2003) Regulation of cell death: The calcium-apoptosis link. *Nat Rev Mol Cell Biol* 4:552–565.
10. Hanson CJ, Bootman MD, Roderick HL (2004) Cell signaling: IP_3 receptors channel calcium into cell death. *Curr Biol* 14:R933–R935.
11. Choe CU, Ehrlich BE (2006) The inositol 1,4,5-trisphosphate receptor (IP_3R) and its regulators: Sometimes good and sometimes bad teamwork. *Sci STKE*, 10.1126/stke.3632006re15.
12. White C, *et al.* (2005) The endoplasmic reticulum gateway to apoptosis by Bcl-X(L) modulation of the $InsP_3R$. *Nat Cell Biol* 7:1021–1028.
13. Chen R, *et al.* (2004) Bcl-2 functionally interacts with inositol 1,4,5-trisphosphate receptors to regulate calcium release from the ER in response to inositol 1,4,5-trisphosphate. *J Cell Biol* 166:193–203.
14. Boehning D, *et al.* (2003) Cytochrome c binds to inositol (1,4,5) trisphosphate receptors, amplifying calcium-dependent apoptosis. *Nat Cell Biol* 5:1051–1061.
15. Khan MT, *et al.* (2006) Akt kinase phosphorylation of inositol 1,4,5-trisphosphate receptors. *J Biol Chem* 281:3731–3737.
16. Collins TJ, Lipp P, Berridge MJ, Bootman MD (2001) Mitochondrial Ca^{2+} uptake depends on the spatial and temporal profile of cytosolic Ca^{2+} signals. *J Biol Chem* 276:26411–26420.
17. Boehning D, Joseph SK (2000) Functional properties of recombinant type I, type III inositol 1, 4,5-trisphosphate receptor isoforms expressed in COS-7 cells. *J Biol Chem* 275:21492–21499.
18. Wagner LE, 2nd, Betzenhauser MJ, Yule DI (2006) ATP binding to a unique site in the type-1 S2- inositol 1,4,5-trisphosphate receptor defines susceptibility to phosphorylation by protein kinase A. *J Biol Chem* 281:17410–17419.
19. Söderberg O, *et al.* (2006) Direct observation *in situ* of individual endogenous protein complexes by proximity ligation. *Nat Methods* 3:995–1000.
20. Kotelevets L, *et al.* (2001) The lipid phosphatase activity of PTEN is critical for stabilizing intercellular junctions and reverting invasiveness. *J Cell Biol* 155:1129–1135.
21. Rizzuto R, Duchen MR, Pozzan T (2004) Flirting in little space: The ER/mitochondria Ca^{2+} liaison. *Sci STKE*, 10.1126/stke.2152004re1.
22. Szabadkai G, *et al.* (2006) Chaperone-mediated coupling of endoplasmic reticulum and mitochondrial Ca^{2+} channels. *J Cell Biol* 175:901–911.
23. Pogue SL, Kurosaki T, Bolen J, Herbst R (2000) B cell antigen receptor-induced activation of Akt promotes B cell survival and is dependent on Syk kinase. *J Immunol* 165:1300–1306.
24. Yule DI, Straub SV, Bruce JI (2003) Modulation of Ca^{2+} oscillations by phosphorylation of Ins(1,4,5)P3 receptors. *Biochem Soc Trans* 31:954–957.
25. Bare DJ, *et al.* (2005) Cardiac type inositol 1,4,5-triphosphate receptor: Interaction and modulation by calcium calmodulin-dependent protein kinase II. *J Biol Chem* 280:15915–15920.
26. Tang TS, *et al.* (2003) Huntingtin and huntingtin-associated protein 1 influence neuronal calcium signaling mediated by inositol-(1,4,5) triphosphate receptor type 1. *Neuron* 39:227–239.
27. Schug ZT, Joseph SK (2006) The role of the S4–S5 linker and C-terminal tail in inositol 1,4,5-trisphosphate receptor function. *J Biol Chem* 281:24431–24440.
28. Patterson RL, Boehning D, Snyder SH (2004) Inositol 1,4,5-trisphosphate receptors as signal integrators. *Annu Rev Biochem* 73:437–465.
29. Pawson T, Scott JD (1997) Signaling through scaffold, anchoring, and adaptor proteins. *Science* 278:2075–2080.
30. Lindsay Y, *et al.* (2006) Localization of agonist-sensitive PtdIns(3,4,5)P_3 reveals a nuclear pool that is insensitive to PTEN expression. *J Cell Sci* 119:5160–5168.
31. Gerasimenko JV, *et al.* (2002) Menadione-induced apoptosis: Roles of cytosolic Ca^{2+} elevations and the mitochondrial permeability transition pore. *J Cell Sci* 115:485–497.
32. Criollo A, *et al.* (2007) Regulation of autophagy by the inositol trisphosphate receptor. *Cell Death Differ* 14:1029–1039.
33. Dufner A, *et al.* (1999) Protein kinase B localization and activation differentially affect S6 kinase 1 activity and eukaryotic translation initiation factor 4E-binding protein 1 phosphorylation. *Mol Cell Biol* 19:4525–4534.
34. Parker AK, Gergely FV, Taylor CW (2004) Targeting of inositol 1,4,5-trisphosphate receptors to the endoplasmic reticulum by multiple signals within their transmembrane domains. *J Biol Chem* 279:23797–23805.
35. Kasri NN, *et al.* (2004) Regulation of $InsP_3$ receptor activity by neuronal Ca^{2+}-binding proteins. *EMBO J* 23:312–321.
36. Wojcikiewicz RJ (1995) Type I, II, and III inositol 1,4,5-trisphosphate receptors are unequally susceptible to down-regulation and are expressed in markedly different proportions in different cell types. *J Biol Chem* 270:11678–11683.
37. Manders EM, *et al.* (1992) Dynamics of three-dimensional replication patterns during the S-phase, analyzed by double labeling of DNA, confocal microscopy. *J Cell Sci* 103:857–862.